

Blocker-related Changes of Channel Density

Analysis of a Three-State Model for Apical Na Channels of Frog Skin

SANDY I. HELMAN and LYNN M. BAXENDALE

From the Department of Physiology and Biophysics, University of Illinois at Urbana-Champaign, Urbana, Illinois 61801

ABSTRACT Blocker-induced noise analysis of apical membrane Na channels of epithelia of frog skin was carried out with the electroneutral blocker (CDPC, 6-chloro-3,5-diamino-pyrazine-2-carboxamide) that permitted determination of the changes of single-channel Na currents and channel densities with minimal inhibition of the macroscopic rates of Na transport (Baxendale, L. M., and S. I. Helman. 1986. *Biophys. J.* 49:160a). Experiments were designed to resolve changes of channel densities due to mass law action (and hence the kinetic scheme of blocker interaction with the Na channel) and to autoregulation of Na channel densities that occur as a consequence of inhibition of Na transport. Mass law action changes of channel densities conformed to a kinetic scheme of closed, open, and blocked states where blocker interacts predominantly if not solely with open channels. Such behavior was best observed in "pulse" protocol experiments that minimized the time of exposure to blocker and thus minimized the contribution of much longer time constant autoregulatory influences on channel densities. Analysis of data derived from pulse, staircase, and other experimental protocols using both CDPC and amiloride as noise-inducing blockers and interpreted within the context of a three-state model revealed that Na channel open probability in the absence of blocker averaged near 0.5 with a wide range among tissues between 0.1 and 0.9.

INTRODUCTION

We address in this paper the issue of blocker-induced noise analysis of apical membrane Na channels in epithelia of frog skin with specific regard to the determination of single-channel Na currents and channel densities that together determine the rates of apical membrane Na entry and hence Na absorption by such tissues. For

Address reprint requests to Dr. Sandy I. Helman, Department of Physiology and Biophysics, University of Illinois, 524 Burrill Hall, 407 South Goodwin Avenue, Urbana, IL 61801. Dr. Baxendale's present address is Houck Hall, Johns Hopkins University, Baltimore, MD 21205.

this purpose we have used a relatively weak electroneutral Na channel blocker (CDPC, 6-chloro-3,5-diamino-pyrazine-2-carboxamide) that has permitted noise analysis with relatively small inhibition of the macroscopic rates of Na transport and at blocker concentrations in a range well below and above its K_B^{CDPC} (Baxendale and Helman, 1986). It was thus possible to determine changes of single-channel currents and channel densities in the vicinity of the spontaneous rates of Na transport and to analyze for kinetic models that could explain the blocker-dependent changes of channel densities (open and blocked states). As will become evident, the blocker-dependent changes of channel density according to mass law action conformed rather well to a simple three-state model of closed, open, and blocked state kinetics in which the blocker interacts predominantly if not solely with open states of the Na channel. In addition to mass law-related changes of channel densities, blocker inhibition of apical Na entry led to secondary long time-constant autoregulation of channel densities (Abramcheck et al., 1985).

Similar studies were carried out with the more potent Na channel blocker amiloride. This however required knowledge of the K_B^{Amil} and led to a new method for its determination (see Results). Microscopic K_B^{Amil} averaged 61 nM and was less in value than K_B^{Amil} measured macroscopically from changes of short-circuit current under similar conditions (Helman et al., 1983). Such findings are expected according to three-state kinetics where blocker interacts principally with open states of the epithelial Na channel. In all groups of studies mean Na channel open probability averaged near 0.5.

GLOSSARY

- I_{sc} short-circuit current; $\mu\text{A}/\text{cm}^2$
 $[B]$ blocker concentration in apical solution; μM
 I_{Na}, I_{Na}^B amiloride inhibitable I_{sc} in the absence or presence of blocker in the apical solution; $\mu\text{A}/\text{cm}^2$
 i_{Na}, i_{Na}^B single-channel Na current in the absence or presence of blocker; pA
 k_{ob} open to blocked state rate coefficient; radians/s · μM
 k_{bo} blocked to open state rate coefficient; radians/s
 K_B equilibrium blocker coefficient of open channels $\equiv k_{bo}/k_{ob}$; μM
 β closed to open state rate coefficient, s^{-1}
 α open to closed state rate coefficient, s^{-1} (also coefficient of $1/f^\alpha$ component of power density spectra [PDS])
 β' open probability in the absence of blocker $\equiv \beta/(\beta + \alpha)$
 N_o, N_o^B open-channel density in the absence or presence of blocker
 N_b density of blocked open channels
 N_{ob} sum of open and blocked open-channel densities; $N_{ob} \equiv N_o^B + N_b$
 N_c, N_c^B density of closed channels in the absence and presence of blocker
 N_{cb} density of blocked closed channels
 N_T, N_T^B total channel density in the absence or presence of blocker
 K_B^C equilibrium blocker concentration of closed channels (see text)
 F relative equilibrium blocker coefficients $\equiv K_B^C/K_B$
 f_c corner frequency (Hz) of current noise PDS
 S_o low frequency plateau value of PDS

MATERIALS AND METHODS

Abdominal skins of *Rana pipiens* (Kons Scientific, Germantown, WI) were used in all experiments. After "scraping" away ~90% of the corium to reduce the unstirred layer at the basolateral surface, the tissues were short-circuited in continuous flow chambers (Abramcheck et al., 1985). Flow rates were ~8 ml/min through chamber volumes of 0.6 ml. Within 2–3 h of continuous short-circuiting, the short-circuit current I_{sc} stabilized to control values. The Ringer's solution contained in millimolar: 100 NaCl, 2.4 KHCO₃, and 2.0 CaCl₂ at a pH near 8.1.

Noise Analysis and Theoretical Considerations

Data acquisition for power density spectral analysis was identical to that described previously (Van Driessche and Zeiske, 1980; Abramcheck et al., 1985). In brief, current noise was digitized by computer and Fourier transformed to give current noise PDS that were fit by non-linear least-squares regression analysis to $1/f^\alpha$ and Lorentzian components according to Eq. 1:

$$S(f) = \frac{S_1}{f^\alpha} + \frac{S_0}{1 + (f/f_c)^2} \quad (1)$$

The PDS were derived from an average of 60 sweeps of data (2,048 points) of either 2- or 1.2-s duration resulting in excellent signal/noise ratio (see Fig. 2).

CDPC (Aldrich Chemical Co., Milwaukee, WI) (see Fig. 1) was used at concentrations between 5 and 200 μ M. The relationship between f_c and $[B]$ (corner frequency plots) was linear (see Results), from which the ON (k_{ob}) and OFF (k_{bo}) rate coefficients for blocker interaction with open channels were determined according to Eq. 2:

$$2\pi f_c = k_{ob} [B] + k_{bo} \quad (2)$$

In the absence of blocker, Lorentzian components were not detectable within a bandwidth of 0.5 and 1,000 Hz, and the PDS were characterized by $1/f^\alpha$ noise at the lower frequencies (Fig. 2 A). When apical membranes were exposed to CDPC, a single Lorentzian appeared in the PDS as shown in Fig. 2 B and C. f_c ranged between ~35 and >220 Hz at [CDPC] between 5 and 200 μ M. Amiloride was used at $[B]$ between 0.5 and 10 μ M. Lorentzian components of the PDS could not be resolved at amiloride concentrations <0.5 μ M, leading therefore to the conduct of amiloride-induced noise analysis at amiloride concentrations considerably greater than the mean K_B^{Amil} of 61 nM (see Results).

From the values of S_0 , f_c , k_{ob} , and the macroscopic rates of apical Na entry J_{Na}^B , the single-channel Na current, i_{Na}^B , was calculated at each blocker concentration (Eq. 3) assuming in accordance with the observed linearity of the corner frequency plots that the rate coefficients reflected only fluctuations of the channels between open and blocked states.

$$i_{Na}^B = \frac{S_0(2\pi f_c)^2}{4J_{Na}^B k_{ob} [B]} \quad (3)$$

The density of open channels at any blocker concentration is by Eq. 4:

$$N_o^B = J_{Na}^B / i_{Na}^B \quad (4)$$

With channels fluctuating between open (N_o^B) and blocked states (N_b) the total pool of channels in open + blocked states (N_{ob}) at any $[B]$ is according to the Law of Mass Action:

$$N_{ob} = N_o^B(1 + [B]/K_B) = N_o^B + N_b \quad (5)$$

where $K_B = k_{bo}/k_{ob}$ of the open-state blocker reaction.

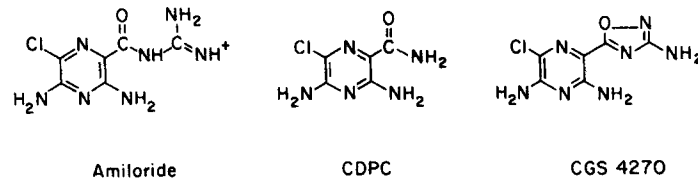


FIGURE 1. Comparison of electroneutral Na channel blockers CDPC and CGS 4270 with cationic amiloride.

In the absence of a closed state (two-state model consisting of open and blocked states), N_{ob} so calculated is the same as the total channel density, N_T , at any $[B]$. In the absence of "recruitment" of channels from any source and by any mechanism during blocker inhibition of I_{sc} , N_{ob} and hence N_T would be expected to remain constant (independent of $[B]$). This however is not the case for experiments carried out with amiloride and CGS 4270 (Helman et al., 1983; Abramcheck et al., 1985), other Na channel blockers (Li and Lindemann, 1983; Li et al., 1985, 1987), nor indeed for CDPC (to be reported below). In principle, blocker-dependent increases of N_{ob} can arise from recruitment of channels by mass law action from a closed state (three-state model, see below) at constant total channel density ($N_T = N_T^B$) provided that blocker binds preferentially to the open state of the channel and not to a closed state of the channel. Blocker-dependent increases of N_{ob} can arise also from recruitment of new, stored, or dormant channels that lead to increases of $N_T^B > N_T$. Hence the general problem is to distinguish between blocker-dependent changes of channel density due directly to mass law action and changes of channel density due to "autoregulation" of channel density, namely, mechanisms other than those related directly to the rate coefficients governing the exchange of channels between closed, open, and blocked states of the channels.

Mass Law Considerations

Patch-clamp experiments indicate unequivocally that highly selective epithelial Na channels fluctuate spontaneously between closed and open states with rather long mean open and closed times of several to many seconds (Sariban-Sohraby et al., 1984; Helman et al., 1985; Palmer and Frindt, 1986; Eaton and Hamilton, 1988; Marunaka Y., and D. C. Eaton, personal communication). In the presence of blocker, channels are distributed among at least

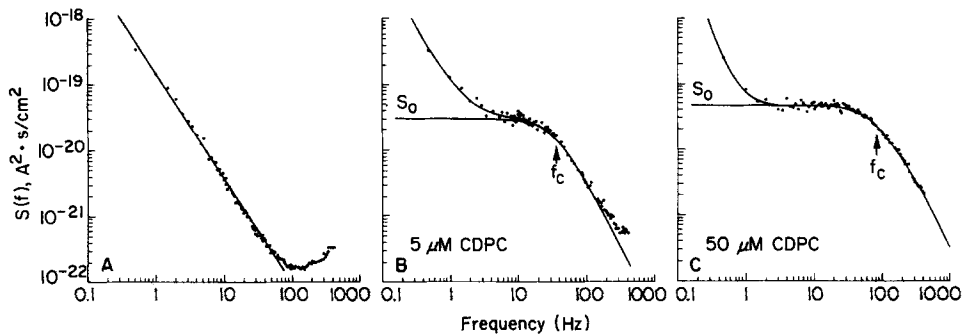
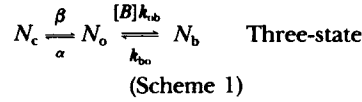


FIGURE 2. Power density spectra of a short-circuited epithelium in the absence (A) and presence of apical $5 \mu\text{M}$ (B) and $50 \mu\text{M}$ (C) CDPC. Corner frequencies, f_c , are shown at the arrows.

three states:



In the absence of blocker the open state probability, β' , is defined by $\beta/(\beta + \alpha)$. In the presence of blocker and its interaction with open states, channels are "recruited" from closed into open and blocked states. Blocker-dependent changes of open-channel density (N_o^B) and open + blocked channel density (N_{ob}) are given by the equations summarized in Table I. For purpose of reference, equations for two- and four-state models are also given in Table I, where it was assumed that N_T is constant at all $[B]$ ($N_T = N_T^B$). It should be noted that N_{ob} would remain constant for all $[B]$ if channels fluctuated alone between an open and blocked

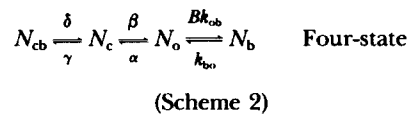
TABLE I
Blocker-dependent Changes of Channel Densities

Normalized density	Two-state $\begin{matrix} Bk_{ob} \\ o \rightleftharpoons b \\ k_{bo} \end{matrix}$	Three-state $\begin{matrix} \beta & Bk_{ob} \\ c \rightleftharpoons o \rightleftharpoons b \\ \alpha & k_{bo} \end{matrix}$	Four-state $\begin{matrix} k_{bo} & \beta & Bk_{ob} \\ cb \rightleftharpoons c \rightleftharpoons o \rightleftharpoons b \\ Bk_{ob} & \alpha & k_{ob} \end{matrix}$
N_o^B/N_o	$\frac{1}{1 + B/K_B}$	$\frac{1}{1 + \beta' B/K_B}$	$\frac{1}{1 + B/K_B}$
N_b/N_o	$\frac{B/K_B}{1 + B/K_B}$	$\frac{B/K_B}{1 + \beta' B/K_B}$	$\frac{B/K_B}{1 + B/K_B}$
N_{ob}/N_o	1	$\frac{1 + B/K_B}{1 + \beta' B/K_B}$	1
N_c^B/N_o	—	$\frac{\alpha/\beta}{1 + \beta' B/K_B}$	$\frac{1 - 1/\beta'}{1 + B/K_B}$
N_{cb}/N_o	—	—	$\frac{(1 - \beta')B/K_B}{1 + B/K_B}$

Blocker-dependent changes of channel densities according to the law of mass action. c, o, b, and cb refer to closed, open, blocked, and closed-blocked states of the channels, respectively. B is blocker concentration. Other symbols are given in the glossary of terms. Shown are equations for a two-state and three-state model where blocker interacts alone with open channels. The four-state model assumed that blocker interacts equally with open and closed states of the channel. Total channel density (N_T) was assumed constant.

state (two-state and four-state model). As this does not occur under any circumstance, and in view of spontaneous fluctuations of channels between open and closed states as observed in patch-clamp records, a two-state model can be dismissed from consideration without further comment.

It has been suggested that amiloride binds equally well to both the open and closed state of the Na channel (Ilani et al., 1984) leading in principle to a four-state kinetic model when channels are exposed to blocker.



Assuming that blocker binds equally well to both open and closed states of the channel, N_{ob}

would be expected to remain constant and independent of $[B]$. As this is not the general observation for any Na channel blocker studied so far, it must be inferred that blocker binding to open states of the channel is preferred over blocker binding to closed states of the channel.¹ Defining $K_B^C = \delta/\gamma$ as the equilibrium coefficient of the blocker reaction with the closed state, and defining $K_B^C/K_B \equiv F$, we find that in general:

$$N_o^B/N_o = [1 + \beta'[B]/K_B + ([B]/FK_B)(1 - \beta')]^{-1} \quad (6)$$

and

$$N_{ob}/N_o = (N_o^B/N_o) \cdot (1 + [B]/K_B) \quad (7)$$

If $K_B^C \gg K_B$ (hence $F \rightarrow \infty$), Eq. 6 reduces to the three-state model where

$$N_o^B/N_o = [1 + \beta'([B]/K_B)]^{-1} \quad (8)$$

and

$$N_{ob}/N_o = (N_o^B/N_o) \cdot (1 + [B]/K_B) \quad (9)$$

Thus, according to mass law considerations, the blocker-dependent changes of N_o^B and N_{ob} as given by the above equations provide a basis for evaluation and interpretation of data with relatively simple models of kinetic interactions of blocker with Na channels. To the extent that changes of channel density due to autoregulatory mechanisms can be avoided or at least minimized, we proceeded to analyze and interpret data in accordance with the expectations of the above models.

Autoregulatory Considerations

It is well known that acute perturbation of Na transport leads to secondary long time-constant transients of the I_{sc} . The mechanisms involved are unknown. In experiments of blocker-

¹ Patch-clamp experiments by Y. Marunaka and D. C. Eaton (personal communication) have examined the blocker interaction of CDPC and amiloride with apical Na channels derived from aldosterone-treated A6 epithelia grown on permeable supports. Their data (manuscript submitted) indicate that unlike amiloride, the existence of CDPC closed-blocked states is at best infrequent and that for all practical purposes, CDPC binds preferentially if not solely to open states of the channel, which is in agreement with the thesis of this paper.

It is curious that amiloride, unlike CDPC, causes the appearance of a high affinity closed-blocked state (Marunaka Y., and D. C., Eaton, manuscript submitted). At least four possibilities may be considered to explain this anomaly: (a) Marunaka and Eaton suggest that because the residency or occupancy time for CDPC in the channel is very short (according to our data ~ 5 ms for CDPC and ~1,000 ms for amiloride), the probability of transition of a blocked channel into a closed-blocked state would be relatively infrequent. (b) Amiloride with a pK_a near 8.7 exists in both cationic and electroneutral forms, thereby exposing the channels to different forms of the blocker with undoubtedly different rate coefficients for binding to open and perhaps closed channels. (c) It has come to our attention that amiloride-like impurities contaminate some commercially available preparations, which would lead to problems in assessing channel kinetics in the face of multiple forms of blocker interactions with the channels. (d) Amiloride at micromolar concentrations penetrates cells exerting influence on cellular enzymes that are involved in regulation of apical membrane permeability to Na and may alter channel kinetics. Such problems are exacerbated especially with amiloride where data must be accumulated over rather lengthy intervals of time and where the stability of the patch is questionable due either to spontaneous decay of patch stability and/or time-dependent changes of regulatory mechanisms influencing channel activity and its interactions with blocker. With high rate blockers like CDPC, such concerns are minimized and may at least in part account for the compatibility of noise and patch experiments, which indicates that blocker kinetics conform to a three-state model where blocker interacts almost exclusively if not solely with open channels.

induced noise analysis using a “staircase” protocol of increasing blocker concentration, the I_{sc} records appear “scalped” with I_{sc} returning toward control values after step increases of blocker concentration. Long time-constant secondary transients of the I_{sc} may reflect time-dependent changes of rate coefficients and/or changes of the total pool of channels (N_T) involved in the blocker reaction. Indeed, such time-dependent changes of channel densities would add to those of N_o^B and N_{ob} due to the mass law expectations indicated above.

To the extent that k_{ob} and k_{bo} of the blocker reaction is independent of time of exposure of the channels to blocker (see below), autoregulatory influences on N_o^B and N_{ob} were expected to be manifest as changes of either β' and/or N_T .

Kinetics of the Blocker Reaction

Long time-constant transient autoregulation of channel density as indicated in Results, is of the order of 10–20 min. Such time constants cannot arise from mass law blocker interaction with the Na channels. If for example the epithelium is exposed to a step increase of blocker concentration, the channels will redistribute among closed, open, and blocked states with time constants related directly to the rate coefficients. For a step increase of [CDPC] from 0 to 5 μ M where f_c is ~ 40 Hz (see Results), the time constant for channel redistribution between open and blocked states is near 4 ms, which for all practical purposes is near instantaneous. Assuming equal mean open and closed times of 5 s for spontaneous fluctuations between closed and open states, the time constant for redistribution of channels between closed and open states is 2.5 s with a corner frequency of 0.06 Hz. Accordingly, equilibrium redistribution of channels after exposure to blocker would occur well within 30 s since it is dictated by the values of α and β . In the absence of evidence to the contrary, we assumed that it was most unlikely that mean open and closed times of Na channels are in the range of 5–10 min as would be necessary to explain long time-constant transients in the range of 10–20 min.

It should be recalled that spontaneous Lorentzians are not observed in the absence of blocker at frequencies >0.1 Hz. Such observations are in agreement with the idea that spontaneous fluctuations between open and closed states occur at a low rate and as such will have little or no influence on the blocker-induced Lorentzians that occur in a range of 30 to >200 Hz (at [CDPC] between 5 and 200 μ M). Thus, it was not surprising that when using Na channel blockers like CDPC the relationship between $[B]$ and $2\pi f_c$ (Eq. 2) was linear, as would be expected when Lorentzian current noise arises solely from blocker-related fluctuations between open and blocked states, which leads directly to the determination of k_{ob} and k_{bo} of the open-state blocker reaction.

Control Parameters

Whereas blocker inhibition of Na transport leads to changes of channel densities and single-channel currents, it remains of particular interest to determine control parameters in the absence of blocker. With weak channel blockers like CDPC, where I_{sc} is perturbed minimally from its control value and where noise analysis is possible at $[B] \ll K_B$, extrapolation of blocker concentration-dependent changes of i_{Na}^B to zero blocker concentration provides a relatively certain method for determination of the control i_{Na} and hence the $N_o = I_{Na}/i_{Na}$. It was moreover apparent, assuming for the moment an ideal three-state model, that the open probability β' in the absence of blocker can be calculated at all $[B]$ after rearrangement of Eq. 8.

$$\beta' = \frac{1 - N_o^B/N_o}{(N_o^B/N_o) ([B]/K_B)} \quad \text{Three-state} \quad (10)$$

If $N_T = N_T^B$, β' is expected to be constant at all $[B]$ with possible values between 0 and 1. As will be shown in Results, data derived from “pulse” experiments that minimized time of

exposure to the blocker were consistent with this idea. When, however, Na transport was inhibited for prolonged durations, apparent open probabilities, to be referred to as " β ", decreased with time of exposure to the blocker reflecting most likely time-dependent changes of N_T^B . In such experiments, the changes of " β " were extrapolated to the zero time and zero blocker concentration control state of the tissue to yield β' of the preblocker control state of the tissue.

In principle, regardless of time and/or other dependencies of the channel densities and single-channel currents, and provided that these parameters were well behaved and minimally perturbed by blocker from their control values, extrapolation to zero blocker concentration was assumed to provide reasonable control parameter values of the apical membrane Na channels, namely, i_{Na} , N_o , and β' . It follows directly that total channel density in the absence of blocker is given by $N_T = N_o/\beta'$.

All experiments were carried out at room temperature (22–27°C), and statistical data are given as means \pm SEM. Standard error bars not appearing in figures are within the size of the data points.

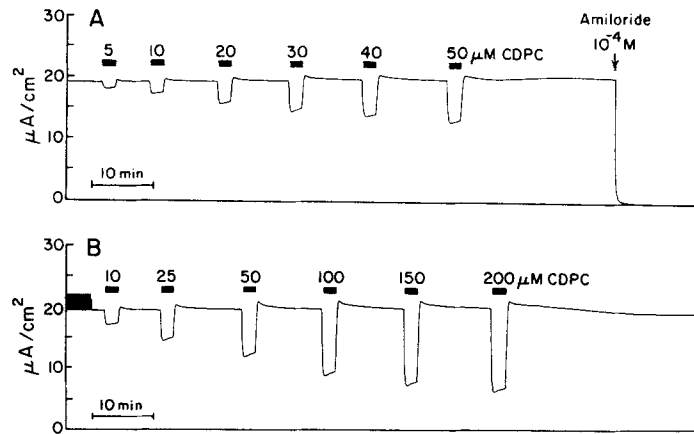


FIGURE 3. Pulse protocol experiments. The changes of I_{Na} are shown for two for typical experiments in response to pulsing the tissues with CDPC for ~ 2 min. Note abrupt changes of I_{Na} upon addition and removal of CDPC from the apical solution and the secondary and slower relaxations of the I_{Na} both during and after pulsing with CDPC. CDPC-induced current noise was measured during the latter 72 s of each pulse (60 sweeps \times 1.2 s/sweep). I_{Na}^B was taken as the mean over this time interval.

RESULTS

Pulse Protocol

The dependency of single-channel Na current (i_{Na}^B) and open-channel density (N_o^B) on blocker concentration was evaluated using two protocols, which will be referred to as pulse and staircase protocols. As illustrated in Fig. 3, tissues were subjected to pulses of CDPC (~ 2 min) at concentrations between 5 and 50 μ M or 10 and 200 μ M. It was evident that CDPC caused abrupt inhibition of the I_{Na} followed by a relatively small relaxation of the I_{sc} towards control. Relatively small transient overshoots of the I_{Na} were observed also upon washout of CDPC from the apical solu-

tion. Between pulses, the I_{Na} relaxed back toward control values. This phenomenon was explored in greater detail (see below).

Current noise spectra were obtained during the last 60 s of each pulse of CDPC and the data were summarized as shown in Fig. 4 and Table II. In 10 experiments CDPC pulses ranged between 5 and 50 μM (Fig. 4, A–D) and in a second group of 8

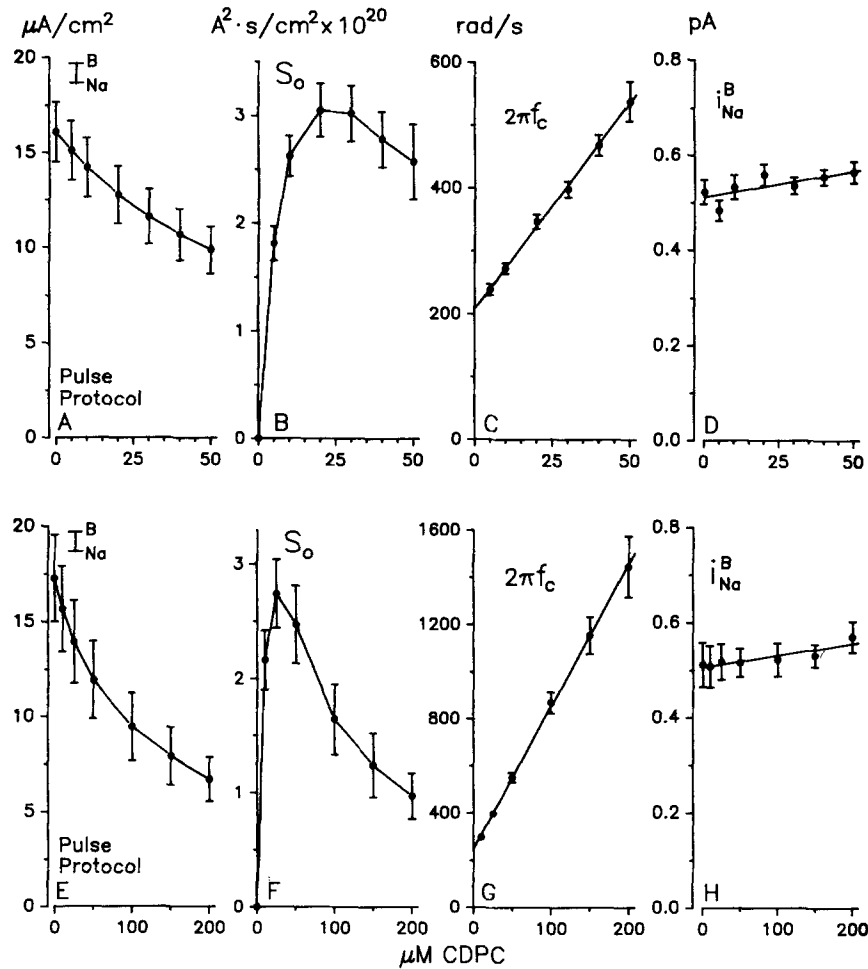


FIGURE 4. Summary data of pulse protocol experiments. 0–50 μM CDPC pulse experiments are shown in panels A–D. 10–200 μM CDPC pulse experiments are shown in E–H. Values are means \pm SEM for all experiments. Analysis of individual experiments provided the data summarized in Table I.

experiments between 10 and 200 μM (Fig. 4, E–H). The amiloride-sensitive macroscopic Na transport (I_{Na}^B) was inhibited progressively by increasing concentration of CDPC while S_o showed the expected biphasic behavior with increasing $[B]$. The corner frequency plots ($2\pi f_c$ vs. $[\text{CDPC}]$) were linear up to 200 μM CDPC from which ON (k_{ob}) and OFF (k_{bo}) rate coefficients were determined for individual experiments

TABLE II
Control Values (*Rana pipiens*)

Protocol	I_{Na} $\mu A/cm^2$	k_{ob} $rad/s \cdot \mu M$	k_{bp} rad/s	K_B μM	i_{Na} pA	N_o millions/ cm^2	β'	N_T millions/ cm^2
Pulse								
0-50 μM CDPC (N = 10)	16.24 \pm 1.60 (9.15-23.78)	6.57 \pm 0.32 (4.59-8.12)	206.9 \pm 6.3 (174.3-237.0)	32.0 \pm 1.7 (26.6-45.5)	0.53 \pm 0.03 (0.42-0.65)	31.9 \pm 4.1 (19.7-53.1)	0.58 \pm 0.05 (0.27-0.77)	63.3 \pm 11.9 (25.5-140.0)
0-200 μM CDPC (N = 8)	17.42 \pm 2.30 (13.20-32.90)	6.27 \pm 0.48 (3.84-8.36)	238.0 \pm 6.9 (210.3-259.1)	40.2 \pm 4.4 (25.6-65.5)	0.52 \pm 0.05 (0.29-0.71)	36.7 \pm 7.3 (23.9-83.4)	0.45 \pm 0.04 (0.28-0.61)	80.1 \pm 14.9 (52.4-192.6)
Staircase								
0-50 μM CDPC (N = 43)	25.95 \pm 1.45 (12.30-53.60)	7.53 \pm 0.12 (6.08-9.09)	212.2 \pm 5.7 (161.5-308.4)	28.2 \pm 0.6 (23.5-38.2)	0.48 \pm 0.01 (0.32-0.62)	56.5 \pm 4.1 (25.7-167)	0.45 \pm 0.03 (0.063-0.791)	151.5 \pm 15.1 (88.2-540.0)

Values are means \pm SEM (range).

and summarized as groups (Fig. 4). Summary values of k_{ob} and k_{bo} are given in Table II together with the equilibrium constant K_B . Notably, the rate coefficients varied significantly among experiments. K_B ranged spontaneously between ~ 26 and $65 \mu\text{M}$ indicating that the rate coefficients governing the blocker reactions are labile and so possibly regulated by hormonal and/or other cytosolic factors (Els, W.J., and S. I. Helman, submitted for publication).

Single-channel Na currents (i_{Na}^B) were calculated at all blocker concentrations (Fig. 4, *D* and *H*). Despite the wide range of $[B]$ and inhibition of I_{Na} , the i_{Na}^B remained fairly constant, tending to increase slightly with increasing $[B]$. In each experiment the i_{Na}^B were extrapolated to the ordinate at zero blocker concentration, yielding values of the i_{Na} (absence of blocker). The i_{Na} values averaged near 0.53 pA , ranged between 0.29 and 0.71 pA , and were similar to those values reported previously where amiloride and CGS 4270 were used as the noise-inducing blocker (Helman et al., 1983; Abramcheck et al., 1985).

Blocker-dependent changes of open-channel density (N_o^B) and open + blocked channel density (N_{ob}) were calculated with Eqs. 4 and 5, respectively. The control open-channel density in the absence of blocker (N_o) was calculated from the quotient I_{Na}/i_{Na} . With I_{Na} averaging $16.24 \mu\text{A}/\text{cm}^2$, N_o averaged $31.9 \times 10^6 \text{ channels}/\text{cm}^2$ (Table II).

The blocker-dependent changes of N_o^B and N_{ob} are summarized in Fig. 5, *A* and *C*, where as shown N_o^B and N_{ob} were normalized to the values of N_o . N_o^B was decreased while N_{ob} was increased progressively from control N_o with increasing blocker concentration. Clearly, N_{ob} was increased markedly above control N_o , indicating that the pool of channels in open and blocked states was not constant and independent of $[B]$. Moreover, it was apparent, as pointed out previously for experiments with CGS 4270 (Abramcheck et al., 1985), that N_o^B/N_o (and I_{Na}^B/I_{Na}) was >0.5 at $[B] = K_B$. This indicates that changes of N_o^B did not follow either a two-state or a four-state model of blocker kinetics, where in the four-state model blocker interacts equally well with open and closed states of the channel.

An apparent open probability " β' " was calculated at each $[B]$ with Eq. 7. The data are summarized as a function of $[B]$ as shown in Fig. 5, *B* and *D*. It should be emphasized that the apparent value " β' " calculated in this manner presumes that total channel density (open + closed + blocked states) remains constant. Indeed, despite relatively large changes of I_{Na}^B , " β' " remained essentially constant, tending to decrease slightly with increasing $[B]$. For each experiment, the " β' " values were extrapolated to the origin at zero blocker concentration to yield values of β' in the absence of blocker. β' averaged 0.58 and 0.45 for the two groups of pulse protocol experiments, showing, however, a large range of values between 0.27 and 0.77 among tissues.

Assuming that β' remained constant at all $[B]$, the expected mass law behavior of N_o^B and N_{ob} according to three-state model kinetics was calculated and is illustrated by the solid lines drawn in *A* and *C* of Fig. 5. The curves fit the data remarkably well with small consistent deviations from ideal behavior at the higher $[B]$ (Fig. 5 *C*). Such deviations from ideal mass law behavior in these pulse experiments is due most likely to relatively small increases of N_T^B , as will be explored further below. To a rather good first approximation, however, the data derived from pulse experiments

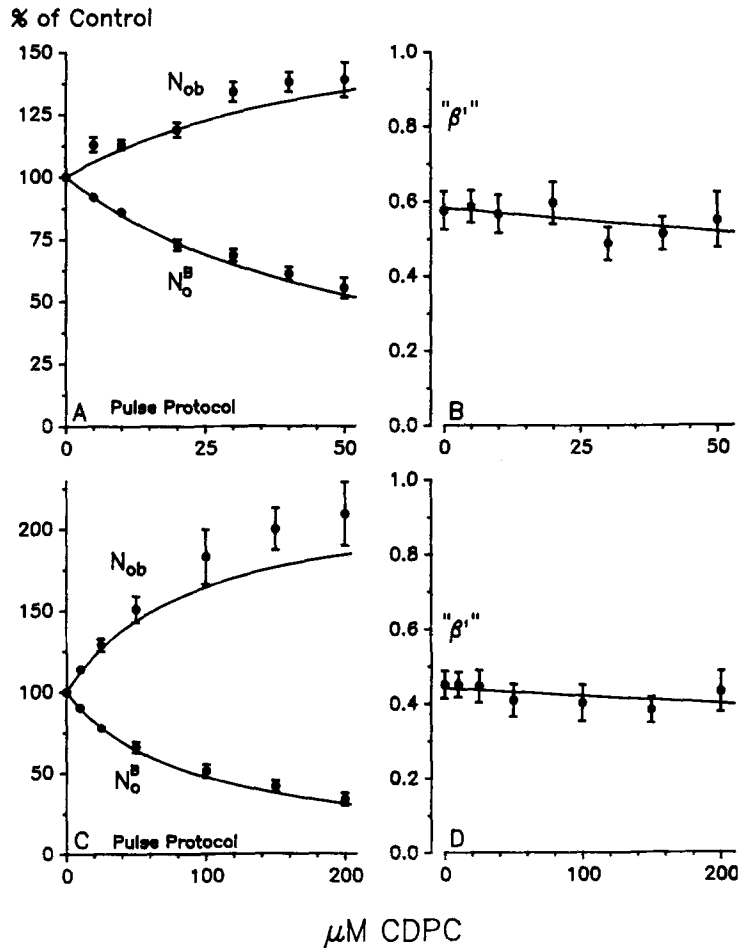


FIGURE 5. Blocker-dependent changes of N_o^B (open channels in the presence blocker) and N_{ob} (open + blocked channels in the presence of blocker) observed in pulse experiments are shown in A (5–50 $\mu\text{M CDPC}$) and C (10–200 $\mu\text{M CDPC}$). An apparent open probability " β' " was calculated at each blocker concentration as shown in B and D (see text). Extrapolation of the apparent " β' " to zero blocker concentration provided estimates of open probability in the absence of blocker (β). The solid lines shown in A and C were drawn using mean β' of 0.58 and 0.45 assuming that $N_T^B = N_T$.

were consistent with channel density kinetics according to a simple three-state model in which blocker interacts predominantly if not solely with open channels. If we accept the idea that N_T^B remained essentially unchanged during brief periods of pulsing with CDPC, then the increases of N_{ob} would reflect "recruitment" of channels from closed into open and blocked states, resulting thereby in the increase of N_{ob} .

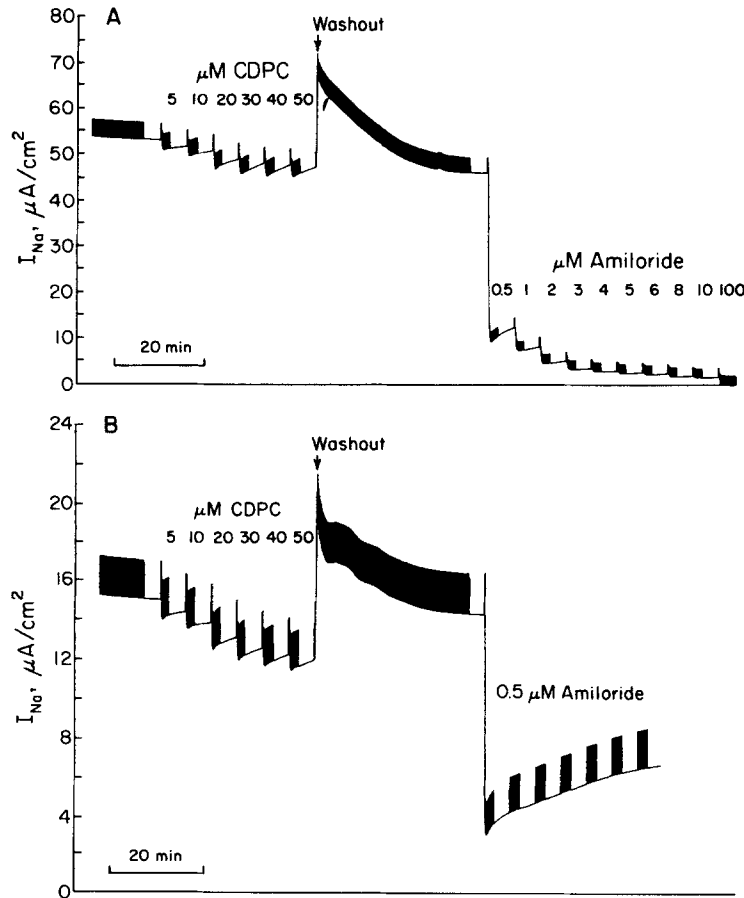


FIGURE 6. Staircase protocol. Typical experiments are shown in A where the I_{Na} was inhibited by a staircase increase of apical solution CDPC concentration. After complete washout of CDPC and secondary relaxation of I_{Na} , the tissue was exposed to a staircase increase of apical solution amiloride concentration. (B) Similar experiments to those of A for CDPC staircase protocol. 0.5 μM amiloride was used to inhibit I_{Na} . Note secondary relaxation of I_{Na} . Current deflection reflects changes of I_{sc} in response to voltage-clamp pulses of a few millivolts. Current noise spectra were measured after turning off the pulse generator.

Autoregulation of Apical Membrane Na Transport

It has been a consistent observation that inhibition of apical Na transport by blockers leads to a secondary transient return of the I_{sc} towards its control value. This has been reported explicitly for studies done with CGS 4270 (Abramcheck et al., 1985) where the I_{sc} records appeared "scalloped" and where, as shown in Fig. 6, similar patterns of scalloping were observed with CDPC and with amiloride at the lowest

concentrations of amiloride that permit blocker-induced noise analysis. With staircase protocols (Fig. 6), where tissues were continuously inhibited by CDPC and with progressively increasing blocker concentrations, complete washout of CDPC from the apical solution was prompt, showing a relatively large overshoot of the I_{Na} and of a magnitude far larger than had ever been observed in the pulse protocol experiments (compare with Fig. 3). It was surmised, as suggested above, that prolonged inhibition of the I_{sc} may have led to an increase of either N_T^B and/or β' . Because f_c remained constant during prolonged exposure to $[B]$ and because the corner frequency plots were linear regardless of the duration of exposure to blocker, it was most unlikely that the scalloped appearance of the I_{sc} records during exposure to blocker could be attributed to changes of the blocker rate coefficients. Moreover, after washout of CDPC, the I_{Na} relaxed toward control rather slowly, indicating that

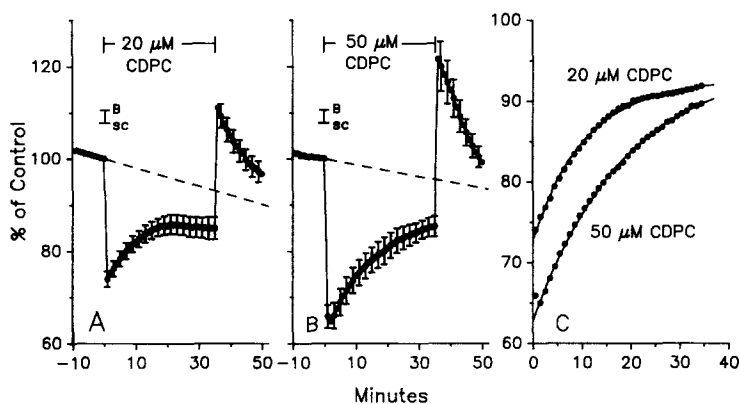


FIGURE 7. Changes of I_{sc} (expressed as a percentage of control) after inhibition by 20 and 50 μ M CDPC. The dashed lines of A and B were used to extrapolate the spontaneous changes of I_{sc} independent of those caused by CDPC. The difference between the observed I_{sc}^B and the extrapolated values was plotted as shown in C and fit to a single exponential (solid line). The mean time constants were 10.9 and 19.0 min for tissues inhibited by 20 and 50 μ M, respectively (see Table II).

changes of either N_T and/or β' were involved in the post-CDPC autoregulatory decrease of I_{Na} .

To obtain a quantitative estimate of the time-dependent changes of the I_{sc} secondary to inhibition by CDPC, two groups of experiments were done (Fig. 7). The I_{sc} was monitored continuously to establish its baseline rate of change with time. At time zero, tissues were exposed to apical solution CDPC at concentrations of either 20 or 50 μ M for 35 min. As with staircase protocols, washout of CDPC from the apical solution resulted in overshoot of the I_{sc} , followed thereafter by a rather slow return towards control values. The control values of I_{sc} (0 time \equiv 100%) and the values of I_{sc}^B at 1 and 35 min after exposure to CDPC are summarized in Table III. To obtain an estimate of the time constant of secondary relaxation of the I_{sc} , the mean data shown in A and B of Fig. 7 were corrected for baseline drift and the

TABLE III
Relaxation of I_{sc} after Inhibition of I_{sc} by CDPC

[CDPC]	I_{sc} control	I_{sc}^B		$\overline{\Delta I_{sc}}$	$\bar{\tau}$	$\overline{I_{sc}(\infty)}$
		1 min	35 min			
	$\mu A/cm^2$	$\mu A/cm^2$	$\mu A/cm^2$	%	min	%
20 μM (7)	13.76 ± 0.35	10.16 ± 0.39	11.74 ± 0.54	19.9	10.9	92.7
50 μM (9)	16.17 ± 1.46	10.40 ± 1.07	13.79 ± 1.37	32.1	19.0	94.9

Values are means \pm SEM.

mean percentage of control values were plotted as shown in C of Fig. 7. These data were fit to a single exponential with time constants of 10.9 and 19.0 min for tissues inhibited by 20 and 50 μM CDPC, respectively (Table II). Expressed as a percentage of control, the magnitudes of the exponentials were 19.9% (20 μM CDPC) and 32.1% (50 μM CDPC), and the values of I_{sc} at $t = \infty$ were 92.7 and 94.9%, respectively. Thus, within 35 min, autoregulatory mechanisms compensate for mass law inhibition of the apical Na channels.

Estimates of β' from Microelectrode Experiments

Experiments were done to assess the time rate of change of the I_{sc} and apical membrane voltage (V_a) in response to apical CDPC, which led to an alternative method for determination of β' . The experimental protocols are illustrated in Fig. 8 with data from typical experiments. V_a and I_{sc} , summarized in Table IV, were normalized to their control values (Fig. 8). 50 μM CDPC caused an abrupt inhibition of I_{sc} with the expected hyperpolarization of V_a (Fig. 8 A). Within 1 min, I_{sc} decreased on average from 34.7 to 25.0 $\mu A/cm^2$, while V_a was hyperpolarized from its mean control value of -81.1 to -93.9 mV. During the following 9 min, both V_a and I_{sc} relaxed towards control values averaging -88.6 mV and 27.5 $\mu A/cm^2$, respectively, at 10 min after exposure to CDPC. Both I_{sc} and V_a exhibited a scalloped appearance when

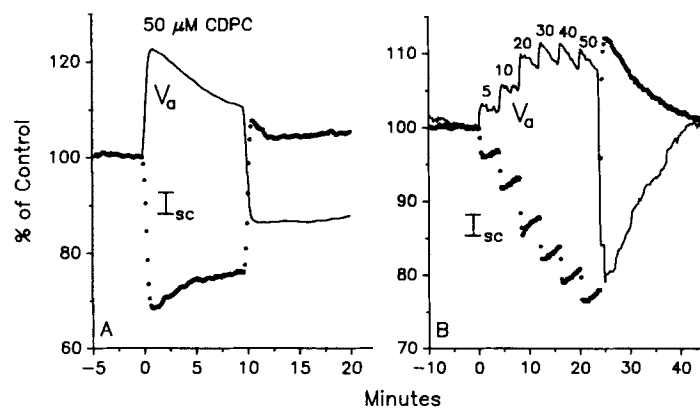


FIGURE 8. Changes of apical membrane voltage (V_a) and I_{sc} after a 50- μM pulse of CDPC (A) and in response to a staircase increase of CDPC concentration (5–50 μM ; B). Note secondary relaxations of both V_a and I_{sc} . Data were normalized to their control values (see Table III) and are shown as a percentage of control.

TABLE IV
Calculation of β' (Microelectrode Experiments)

Protocol	Time min	I_n $\mu A/cm^2$	fR_s	V_s mV	I_n^b/I_n	V_n/V_s^b	β'
Pulse (10)							
Control		34.7 ± 4.8	0.812 ± 0.027	-81.1 ± 5.2	0.705 ± 0.030	0.863 ± 0.016	0.379 ± 0.040
50 μM CDPC	~1	25.0 ± 3.9	0.907 ± 0.021	-93.9 ± 5.6			
Washout CDPC	10	27.5 ± 4.4	0.884 ± 0.021	-88.6 ± 5.6	0.731 ± 0.705	0.851 ± 0.018	0.359 ± 0.041
	~1	36.9 ± 5.2	0.792 ± 0.024	-75.6 ± 5.0			
Staircase (10)							
Control		32.8 ± 3.4	0.817 ± 0.025	-86.0 ± 5.2	0.706 ± 0.026	0.824 ± 0.034	0.419 ± 0.046
5-50 μM CDPC	~25	24.0 ± 2.9	0.888 ± 0.019	-91.8 ± 5.5			
Washout CDPC	~1	33.2 ± 3.6	0.789 ± 0.039	-76.9 ± 5.7			

Values are means ± SEM. See text for calculation of β' .

tissues were subjected to a staircase increase of [CDPC] between 5 and 50 μM (Fig. 8 B). As the initial changes of V_a and I_{sc} occurred rapidly (<1 min) relative to the secondary long time-constant transients, it was assumed in the following calculations that the initial changes of V_a and I_{sc} reflected changes of N_o^B and i_{Na}^B at essentially constant N_T .

Since $I_{sc} = (i_{Na} \cdot N_o)$ and $I_{sc}^B = (i_{Na}^B \cdot N_o^B)$, Eq. 8 can be rewritten as:

$$(I_{sc}^B/I_{sc}) \cdot (i_{Na}/i_{Na}^B) = [1 + \beta'([B]/K_B)]^{-1} \quad (11)$$

At the negative V_a reported in Table IV and with intracellular Na concentration averaging near 14 mM (Rick et al., 1978; Stoddard and Helman, 1985), it is readily shown that:²

$$i_{Na}/i_{Na}^B \approx V_a/V_a^B \quad (12)$$

Substituting V_a/V_a^B for i_{Na}/i_{Na}^B in Eq. 11

$$\beta' \approx \frac{1 - [(I_{sc}^B/I_{sc})(V_a/V_a^B)]}{(I_{sc}^B/I_{sc})(V_a/V_a^B)([B]/K_B)} \quad (13)$$

Mean ratios of V_a/V_a^B and I_{sc}^B/I_{sc} at 1 min after washin and washout of CDPC from the apical solution are reported in Table IV for the 10-min pulse experiments, and for washout of CDPC of the staircase protocol experiments. The mean values of β' were 0.379 and 0.359 at the beginning and end, respectively, of the 10-min pulse experiments and 0.419 at the end of the 25-min staircase experiments (Table IV). Taking into account the spontaneous variability of β' amongst tissues, these mean values of β' are remarkably similar to those of the blocker noise pulse experiments (see above). The constancy of β' near 0.37 would indicate that β' remained unchanged during the inhibition of apical Na entry by 50 μM CDPC for 10–25 min. The inference from these experiments was that long time-constant transients of the I_{sc} were due to time-dependent changes of N_T^B and not to changes of β' .

Time Course Experiments

To test this idea further, experiments were done as illustrated in Fig. 9. During a control period (not shown) epithelia were subjected to CDPC noise analysis for determination of the CDPC rate coefficients and hence K_B . Thereafter, each tissue was exposed to 5 μM CDPC for ~ 30 min before increasing apical [CDPC] abruptly from 5 to 50 μM . PDS were obtained at intervals of 2 min during the 5 μM CDPC control period and thereafter for 30 min after the change to 50 μM CDPC. This protocol permitted calculation of the changes of i_{Na}^B , N_o^B , and N_{ob} after abrupt inhibition of the macroscopic I_{Na}^B . As shown in A of Fig. 9, the I_{Na}^B exhibited a secondary long time-constant transient similar to that reported above. The i_{Na}^B increased abruptly upon inhibition of I_{Na}^B and is due most likely to the concurrent hyperpolarization of V_a . The i_{Na}^B also showed a secondary long time-constant transient which is associated with secondary depolarization of V_a (see Fig. 8 A).

² For perfect Goldman rectification (Goldman, 1943; Palmer, 1984) and assuming little or no change of intracellular Na concentration during abrupt changes of V_a , this approximation introduces at most a 2% error. At the extreme V_a of -76.9 and -91.8 mV (see Table IV), V_a/V_a^B is 0.838 and i_{Na}/i_{Na}^B is 0.852.

The changes of N_o^B and N_{ob} are summarized in Fig. 9 B. Acute increase of [CDPC] from 5 to 50 μM caused within 2 min abrupt changes of N_o^B and N_{ob} , followed thereafter by long time-constant increases of both N_o^B and N_{ob} . Notably, and in comparison with data obtained in pulse experiments, the long time-constant changes of N_o^B and N_{ob} were relatively small during the first 2 min after step increase of blocker concentration. We take this as evidence in support of the idea that blocker-related changes of channel densities that occur acutely reflect primarily if not solely the mass action of the blocker to reduce open-channel density. Indeed, it appeared that changes of channel density due to mass action and due to autoregulatory influences could be separated because of the large difference in time constants associated with these processes.

If indeed N_T^B increased progressively with time after inhibition of I_{Na} , then accord-

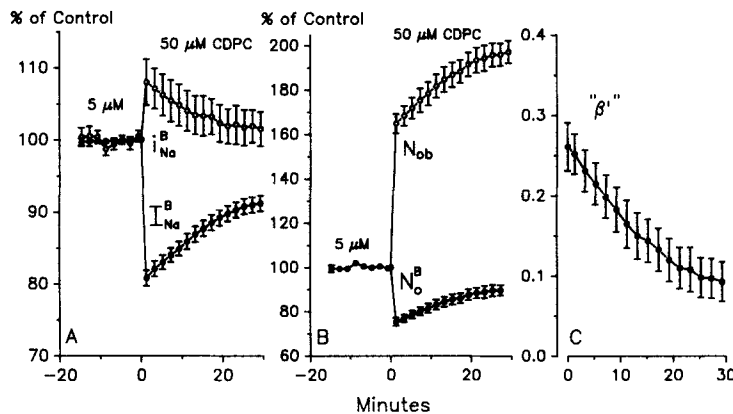


FIGURE 9. Time course experiments. Tissues were exposed to a step increase of CDPC concentration. Current-noise spectra were obtained at intervals of 2 min. Note immediate changes of I_{Na}^B , I_{Na}^B , N_o^B , and N_{ob} followed by secondary long time-constant transients. Data were normalized to their control values (5 μM CDPC) and are shown as a percentage of control (A and B). Changes of the apparent β' are shown in C, which most likely reflects time-dependent increases of N_T^B . Extrapolation of the β' to zero time gave $\beta' = 0.26 \pm 0.03$ (see text).

ing to Eq. 10, the β' was expected to underestimate β' (due to time-dependent increases of N_o^B). As shown in Fig. 9 C, β' decreased continuously with time after step inhibition of I_{Na}^B . β' was calculated with Eq. 16 below recognizing that N_o^B were measured at 5 and 50 μM CDPC. At these concentrations of CDPC:

$$N_o^5/N_o = [1 + \beta'(5/K_B)]^{-1} \quad (14)$$

and

$$N_o^{50}/N_o = [1 + \beta'(50/K_B)]^{-1} \quad (15)$$

Hence

$$\beta' = \frac{1 - (N_o^{50}/N_o^5)}{[(N_o^{50}/N_o^5) \cdot 50/K_B] - (5/K_B)} \quad (16)$$

Extrapolation of the “ β ” to the ordinate (zero $[B]$ and also zero time) gave β' of 0.26 ± 0.03 for this group of experiments.

Staircase Protocol

Blocker-induced noise analysis of epithelia has to our knowledge been carried out exclusively using a staircase protocol (Fig. 6) of increasing blocker concentration. This protocol has the advantage of requiring less time to obtain corner frequency

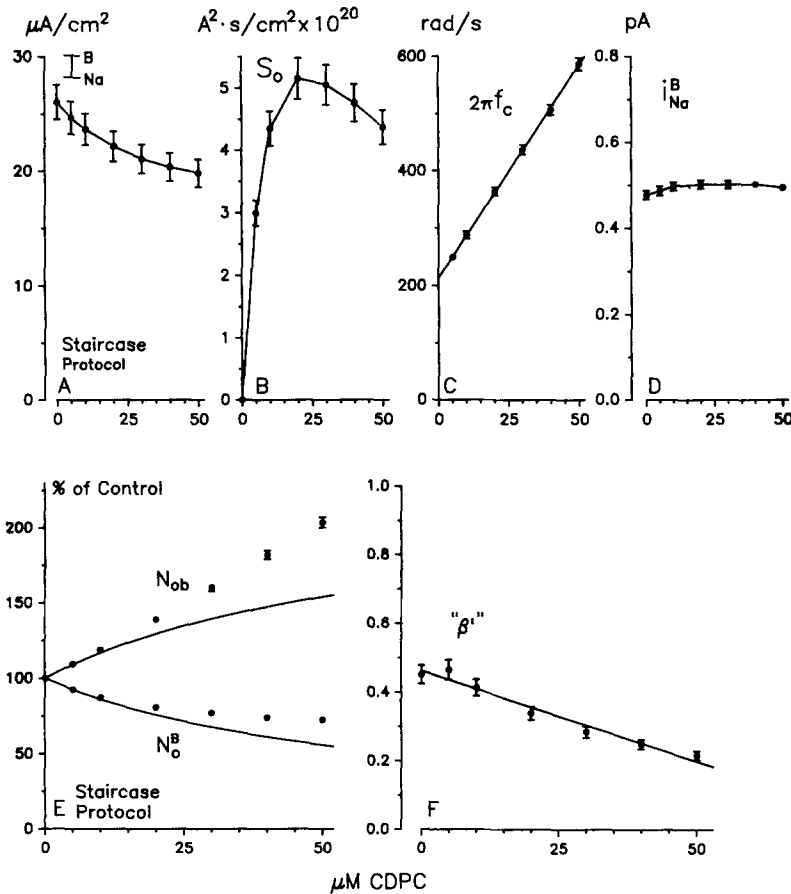


FIGURE 10. Summary of staircase protocol experiments. Compare with Figs. 4 and 5 (see text).

plots (as compared with a pulse protocol) but is disadvantageous insofar as the tissues are subjected to graded and prolonged inhibition of I_{Na} with attendant autoregulatory changes of channel densities. Noting this complication especially with regard to assessing blocker-dependent changes of channel densities and hence determination of β' , a summary of blocker-dependent changes of measured and calculated parameters for 43 tissues is shown in Fig. 10. I_{Na} was decreased from a mean control of 26.05 ± 1.51 to $19.80 \pm 1.21 \mu A/cm^2$ at $50 \mu M$ CDPC or on average to 76.0% of

the control value. In comparison, 50 μM CDPC in the pulse protocol noise experiments caused I_{Na} to decrease on average to 61.4% of the control value. In staircase protocol experiments where the I_{Na} was inhibited by CDPC for ~ 35 min (and at progressively increasing $[B]$) the long time-constant increases of N_{T}^{B} would be expected to result in lesser inhibition of the I_{Na} at 50 μM CDPC, as observed here, and as compared with results of the pulse protocol experiments. The corner frequency plots (Fig. 10 C) were linear in each experiment yielding ON- and OFF-rate coefficients in a range similar to those observed in the pulse protocol experiments (see Table II). i_{Na} averaged 0.48 pA and was the same as in the pulse protocol experiments. The mean i_{Na}^{B} remained essentially constant with increases of $[B]$ (Fig. 10 D) as would be expected with near constancy of V_{a} (Fig. 8 B).

The mean N_{o} of this group of tissues averaged 56.6×10^6 channels/cm² at a mean I_{Na} of 25.95 $\mu\text{A}/\text{cm}^2$ (Table I). In comparison with pulse protocol experiments (Fig. 5 A) and as summarized in Fig. 10 E, the blocker-dependent decreases of N_{o}^{B} were less, and the increases of N_{ob} were greater than those of pulse protocol experiments, especially at the higher $[B]$, where the I_{Na} was inhibited for the longest periods of time.

Noting again that β' , as calculated with Eq. 10, is subject to error owing to time-dependent increases of N_{T} , the " β " values shown in Fig. 10 F were extrapolated to the ordinate to obtain β' . β' averaged 0.45 (Table I, Fig. 10 F). In the absence of time-dependent increases of N_{T} , the solid curves drawn in Fig. 10 E (using a mean β' of 0.45) would represent the expected mass action changes of N_{o}^{B} and N_{ob} with increasing $[B]$. At the lower $[B]$ and for the shorter durations of inhibition of I_{Na} , the N_{o}^{B} and N_{ob} followed rather closely such theoretical expectations for a three-state model. However, as indicated clearly in Fig. 10 E and in contrast to the results of pulse protocol experiments, significant deviations of N_{o}^{B} and N_{ob} were observed in these staircase protocol experiments at the higher $[B]$ and during longer durations of inhibition of I_{Na} . Notably, similar behavior of blocker-dependent changes of N_{ob} was reported for experiments done with CGS 4270 and amiloride (Abramcheck et al., 1985). Such phenomena are therefore unrelated to the specific characteristics of the blocker used to induce blocker noise.

K_B of Amiloride

It has been impossible to determine with adequate certainty the microscopic K_{B} for amiloride due to the very low value of its OFF-rate coefficient, k_{bo} (Helman et al., 1983; Abramcheck et al., 1985). Because it was important to know the value of $K_{\text{B}}^{\text{Amil}}$ for the evaluation of blocker-dependent changes of channel densities, a new method was devised to determine $K_{\text{B}}^{\text{Amil}}$. It was assumed that any blocker of the Na channels would cause the same inhibition of the I_{sc} when used at the same B/K_{B} . Thus for the same fractional inhibition of I_{sc} by any pair of blockers, namely, CDPC and amiloride:

$$\frac{[\text{Amil}]}{K_{\text{B}}^{\text{Amil}}} = \frac{[\text{CDPC}]}{K_{\text{B}}^{\text{CDPC}}} \quad (17)$$

Since amiloride and CDPC concentrations are known and since $K_{\text{B}}^{\text{CDPC}}$ is determined easily and with certainty from corner frequency plots, $K_{\text{B}}^{\text{Amil}}$ could be calcu-

lated with Eq. 17 at the concentration of amiloride that gave the same fractional inhibition of I_{sc} that was caused by CDPC.

Calculation of K_B^{Amil} was done with data obtained in pulse protocol experiments. Epithelia were exposed first to CDPC pulses at concentrations between 10 and 200 μM yielding the empirical relationship between B/K_B^{CDPC} and I_{sc}^{CDPC}/I_{sc} (Fig. 11 A). This was followed by a second series of amiloride pulses at concentrations between 0.02 and 0.4 μM yielding the relationship between [Amil] and I_{sc}^{Amil}/I_{sc} (Fig. 11 B). This range of [Amil] gave fractional inhibitions of I_{sc} similar to those encountered with CDPC. Knowing the I_{sc}^B/I_{sc} at each amiloride concentration and knowing the B/K_B at the same I_{sc}^B/I_{sc} determined previously with CDPC, the K_B^{Amil} was calculated as a function of increasing [Amil] (Fig. 11 C). K_B^{Amil} was on average independent of [B]. In 12 such experiments (Table V), K_B^{Amil} ranged between 44 and 88 nM and

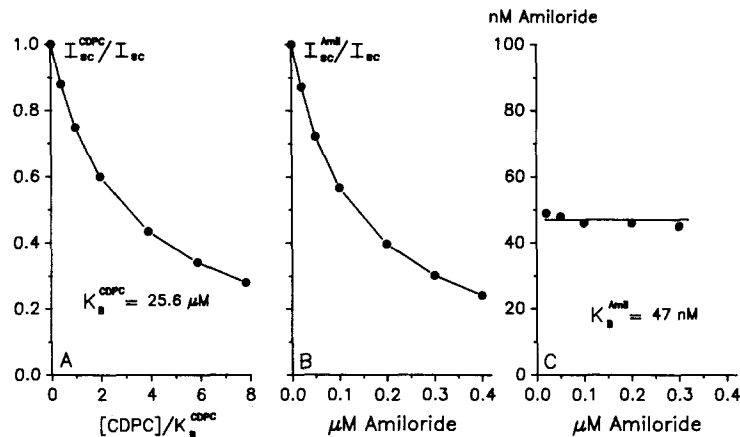


FIGURE 11. Determination of K_B^{Amil} . Tissues were pulsed with either CDPC (10–200 μM) or amiloride (0.02–0.4 μM) to determine the fractional inhibition of I_{sc} . (A) Fractional inhibition of I_{sc} plotted against $[B]/K_B$ for CDPC. K_B^{CDPC} in this experiment was 25.6 μM . (B) Inhibition of I_{sc} plotted against apical solution amiloride concentration. (C) Calculation of K_B^{Amil} as a function of [Amil] according to Eq. 17. Solid line is mean value of 47 nM. As an example calculation, 0.1 μM gave an I_{sc}^{Amil}/I_{sc} of 0.566 (B). $[B]/K_B$ for CDPC was 2.16 (A) at this I_{sc}^{Amil}/I_{sc} . Hence, $K_B^{Amil} = 0.1 \mu\text{M}/2.16 = 46.3 \text{ nM}$.

averaged $61 \pm 4 \text{ nM}$ (pH ~ 8.1). Since the ON-rate coefficient k_{ob}^{Amil} averaged $18.7 \pm 0.6 \text{ rad/s} \cdot \mu\text{M}$ (Table V), the OFF-rate coefficient k_{bo}^{Amil} was calculated to be 1.14 rad/s. It is thus not surprising that k_{bo}^{Amil} cannot be measured with certainty at the ordinate of corner frequency plots.³ For the groups of amiloride experiments

³ With a pK_a of nearly 8.7, $\sim 80\%$ of amiloride is in its active cationic form, and the rate coefficients of the blocker reaction are voltage dependent (Palmer, 1984; Warncke and Lindemann, 1985). k_{bo}^{Amil} of the blocker reaction would therefore be expected to be of lower value in our studies as compared with K-depolarized epithelia where V_a is markedly depolarized from its control value. This undoubtedly contributes to the difficulty in determination of k_{bo}^{Amil} from corner frequency plots of non-K-depolarized tissues as studied here and previously (Helman et al., 1983; Abramcheck et al., 1985). It should be noted also that k_{ob}^{Amil} and k_{bo}^{Amil} as reported here are not corrected either for voltage or pK_a . Accordingly, extrapolation of these values to other conditions must be done with caution.

reported below k_{bo}^{Amil} extrapolated at the ordinate of the amiloride corner frequency plots averaged 4.96 ± 1.31 rad/s (Table VI) or about four times larger than the more likely value of 1.14.

Amiloride-dependent Changes of i_{Na} , N_o , and N_{ob}

Because of the widespread interest in amiloride as a Na channel blocker, it was of interest to evaluate the amiloride-dependent changes of i_{Na}^B and the channel densities with the experimental protocols given in Fig. 6. The control blocker-dependent parameters were evaluated first with CDPC-induced noise. This was followed by either a staircase protocol of amiloride inhibition of I_{Na} (Fig. 6 A) or a time course protocol inhibition of I_{Na} (Fig. 6 B). To be noted in Fig. 6 B was the secondary long time-constant transient of the I_{Na} upon exposure of tissues to $0.5 \mu\text{M}$ amiloride that was also apparent in the scalloped appearance of the I_{Na} record of Fig. 6 A especially at the lower amiloride concentrations.

TABLE V
 K_B^{Amil} as Determined with Reference to K_B^{CDPC}

Expt. No.	K_B^{Amil}
	<i>nM</i>
1	51 ± 2
2	59 ± 3
3	46 ± 2
4	54 ± 4
5	68 ± 1
6	83 ± 1
7	63 ± 1
8	88 ± 2
9	47 ± 1
10	63 ± 2
11	63 ± 1
12	44 ± 1
Mean ± SEM	61 ± 4

The CDPC-derived control data are summarized in Table VI. Pre-amiloride control values of I_{Na} , N_o , and i_{Na} are also summarized in Table VI. The pre-amiloride I_{Na} was measured immediately before the addition of amiloride ($0.5 \mu\text{M}$) to the apical solution. N_o was calculated from the quotient of the pre-amiloride I_{Na} and the i_{Na} determined with CDPC; these values served as controls for the i_{Na}^B and N_o^B measured with amiloride-induced noise. i_{Na}^B was calculated with Eq. 3 at the respective concentrations of amiloride using the measured k_{ob}^{Amil} that averaged 18.7 ± 0.6 rad/s· μM (Table VI).

The blocker-dependent changes of I_{Na}^B , i_{Na}^B , N_o^B , and N_{ob} observed in staircase protocol experiments are summarized in Fig. 12. As shown in Fig. 12 A, amiloride caused the i_{Na}^B to increase on average by ~30%. A similar hyperpolarization of V_a has been observed consistently in microelectrode studies of apical membrane voltage in response to amiloride inhibition of Na entry (Helman and Fisher, 1977). N_o^B decreased markedly from control at $0.5 \mu\text{M}$ amiloride and higher concentrations

TABLE VI
Summary Data for Amiloride Experiments

Protocol	GDPC						Pre-amiloride controls				Amiloride		
	I_{Na} $\mu A/cm^2$	k_{ho} $rad/s \cdot \mu M$	k_{bo} rad/s	K_B μM	i_{Na} pA	N_0 $\times 10^6/cm^2$	β'	I_{Na} $\mu A/cm^2$	N_0 $\times 10^6/cm^2$	k_{ho} $rad/s \cdot \mu M$	k_{bo} rad/s	$*K_B$ μM	β'
Staircase ($N = 7$)	28.47 ± 6.11	6.66 ± 0.29	193.8 ± 5.3	29.5 ± 1.6	0.508 ± 0.052	67.1 ± 19.2	0.44 ± 0.09	28.80 ± 5.15	68.1 ± 16.3	18.7 ± 0.6	4.96 ± 1.31	0.273 ± 0.076	0.47 ± 0.09
Time course ($N = 5$)	18.40 ± 1.33	6.93 ± 0.17	181.7 ± 6.8	26.2 ± 0.8	0.469 ± 0.012	39.1 ± 2.2	0.41 ± 0.10	16.59 ± 1.09	38.9 ± 3.7	—	—	—	0.50 ± 0.05

Values are means \pm SEM.
*Included in this table are values of k_{ho}^{Amil} and K_B^{Amil} determined from the [amiloride] $^{-2}$ πf_c corner frequency plots. Although no negative values of k_{ho} were observed in this group of experiments, the values of k_{ho}^{Amil} and K_B^{Amil} so measured are considered to be unreliable (see text).

(Fig. 12 *B*). N_{ob} increased markedly above control averaging near 700% of control at 10 μM amiloride (Fig. 12 *C*). As with the CDPC staircase protocol experiments, the apparent " β " fell progressively with increasing $[B]$ (Fig. 12 *D*), with β' extrapolated to the ordinate averaging 0.45. The solid lines in *B* and *C* of Fig. 12 were drawn according to Eqs. 8 and 9 assuming that N_T^B remained unchanged from the control N_T . As with CDPC staircase protocol experiments, marked deviation from ideal three-state model behavior was observed with deviation from ideal behavior being far greater than that observed with CDPC inhibition of I_{Na} and due most likely to the much larger inhibition of I_{Na} caused by amiloride. Indeed, at these high amiloride concentrations where $[B]/K_B$ is greater than ~ 2 , the N_{ob} would approach a "saturating" value with a limit equal to the N_T (absence of blocker). For a β' of 0.45, this value is 222% of control provided $N_T^B = N_T$. Clearly the calculated N_{ob} far exceeds such an expectation, leading to the same conclusion as above, namely that increases

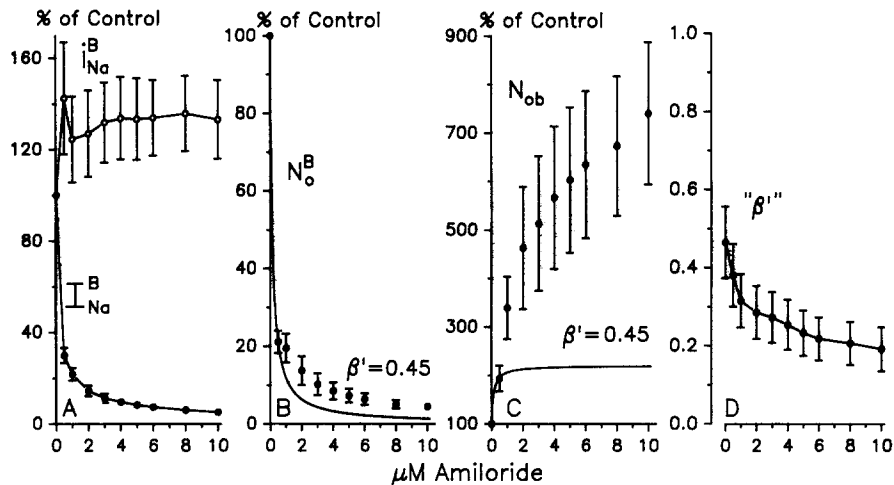


FIGURE 12. Summary of staircase protocol experiments of amiloride-induced noise. Data are normalized to the pre-amiloride control values (Table V).

of N_T^B during secondary long time-constant transients contribute to the pool of channels in open and blocked states.

Time course experiments with amiloride, summarized in Fig. 13, led again to the same conclusion. Acute inhibition of I_{Na} by 0.5 μM amiloride caused a similar increase of i_{Na}^B (compare with Fig. 12 *A*) that remained elevated above control for the 38-min experimental period (Fig. 13 *A*). N_o^B showed an immediate decrease to $\sim 22\%$ of control followed by a secondary long time-constant increase of the N_o^B (Fig. 13 *B*). N_{ob} increased markedly and progressively with time despite the constancy of amiloride concentration in the apical solution (Fig. 13 *C*). The apparent " β " fell progressively with time, and the β' extrapolated to the ordinate averaged 0.50. On the premise again that the secondary changes of N_o^B and N_{ob} reflected long time-constant autoregulation of apical Na entry acting through increases of N_T^B , it was remarkable to observe at the shorter time intervals after exposure to amiloride (~ 3

min) that N_o^B and N_{ob} were not far different from values expected at $0.5 \mu\text{M}$ amiloride at a mean β' of 0.5 in this group of experiments. Accordingly, we conclude that amiloride, like CDPC, caused changes of N_o^B and N_{ob} in accordance with a three-state model of closed, open, and blocked state kinetics, and, moreover, amiloride, like CDPC, binds predominantly if not solely to open channels.

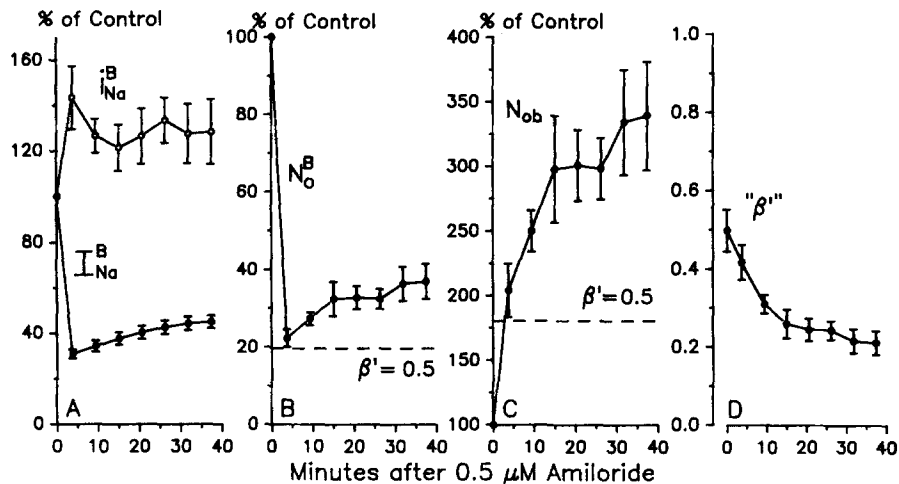


FIGURE 13. Summary of time course experiments after exposure of tissues to $0.5 \mu\text{M}$ amiloride. Data are normalized to the pre-amiloride control values (Table V).

DISCUSSION

An ultimate description of Na absorption by epithelial cells will require detailed knowledge of the regulation of apical membrane channel density and channel kinetics. In this regard, we have turned to blocker-induced noise analysis of the highly selective Na channels of frog skin using the electroneutral Na channel blocker CDPC. Being electroneutral and thus insensitive to change of apical membrane voltage, and lacking a pK at physiological pHs of interest, CDPC, unlike amiloride and other numerous charged analogues, is advantageous in design and interpretation of data obtained from blocker-induced noise analysis. As CDPC-induced Lorentzian-type noise is easily measurable under conditions of minimal inhibition of the macroscopic rates of Na entry, its utility is obvious in assessing Na channel behavior at or very near normal spontaneous rates of Na transport. We have taken advantage of these properties of CDPC to study the changes of single-channel Na currents and Na channel densities that occur with inhibition of apical Na entry.

To our knowledge, no evidence has emerged to indicate that single-channel currents are different when measured with different blockers of the Na channels. Indeed, in the paired experiments using both CDPC and amiloride, the increases of i_{Na}^B caused by amiloride were similar to those expected to result from the hyperpolarization of V_a . Moreover, taking into account the dependency of i_{Na} on V_a , with V_a varying between individual tissues and among species of tissues, the values of i_{Na} are

remarkably similar to those of highly selective Na channels studied by patch clamp (Palmer and Frindt, 1986; Eaton and Hamilton, 1988; Marunaka, Y., and D. C. Eaton, personal communication). Accordingly, despite vast differences in rate coefficients among blockers and the difference of inhibition of I_{Na} by blockers, it seems reasonable to conclude that blockers like CDPC act as probes of the open Na channel with no measurable change of its intrinsic properties. In accordance with this thesis is the consistent observation of linear corner frequency plots of CDPC, like those of other blockers, which argues, moreover, in favor of the idea that the f_c arises alone from blocker interaction with open channels being measurably uninfluenced by other kinetic reactions—notably spontaneous fluctuations between open and closed states of the channel.

With minimal inhibition of the macroscopic rates of Na entry and with minimal change of V_a , extrapolation of the i_{Na}^B to zero blocker concentration gave values of i_{Na} , which when taken together with the I_{Na} , gave values for the open channel density, N_o . i_{Na} averaged near 0.5 pA with significant variability amongst tissues. This at least in part reflects differences of apical membrane voltage and intracellular Na concentration. Assuming a mean V_a of -80 mV and cellular Na concentration of 14 mM, the single-channel Na conductance is in the vicinity of 3.8 pS (chord) or 6.3 pS (slope). Such values are similar to those previously reported that were determined by noise analysis (Helman et al., 1983), analysis of highly selective Na channels reconstituted into lipid bilayers (Sariban-Sohraby et al., 1984), and by patch clamp (Palmer and Frindt, 1986; Eaton and Hamilton, 1988; Marunaka, Y., and D. C. Eaton, personal communication). Although not shown in detail, it was quite apparent that a relationship existed between N_o and I_{Na} over large ranges of spontaneous rates of Na transport encountered among tissues (see Tables II and VI). At a mean I_{Na} of $25.95 \mu\text{A}/\text{cm}^2$, N_o averaged 56.5 million open channels/ cm^2 or ~ 56 channels/cell, or about a single channel per $2 \mu\text{m}^2$ of apical membrane area. At such Na transport rates, it would thus be surprising to find more than one open channel in a patch of apical membrane of $1\text{--}2 \mu\text{m}^2$ unless channels existed in clusters.

Blocker Concentration Dependence of Channel Densities

Availability of CDPC permitted an analysis of the dependence of open-channel density and open + blocked channel density on blocker concentration in a range of concentrations well below and above its K_B , which averaged near $30 \mu\text{M}$. Without exception open-channel density decreased while open + blocked channel density increased from the control N_o with progressive increases of $[B]$. Such behavior is incompatible with the idea of a two-state model of open and blocked channels (see Methods), and indeed some form of "recruitment" is necessary to explain blocker concentration-dependent increases of N_{ob} . Similar observations were made with electroneutral CGS 4270, cationic amiloride, and triamterene as blockers (Baxendale and Helman, 1986). Therefore, such phenomena did not seem attributable to the specific noise-inducing blocker. If the blockers interacted equally well with open and closed states of the channel as had been suggested (Ilani et al., 1984), then according to the four-state scheme of Table I, N_{ob} would have remained independent of $[B]$, and N_o^B would have decreased to 50% of the N_o at $[B]/K_B = 1.0$. As such behavior was never observed in our own experiments or in those of Marunaka and

Eaton (personal communication), we conclude that neither a two-state nor a four-state model of equal blocker interaction with open and closed channels satisfies the empirical observations.

Complicating the analysis and interpretation of the data is the existence of long time-constant transients of the I_{Na} that appear after inhibition of Na entry. We attempted therefore to separate those changes of channel density due to mass law effect from those that occur by so-called autoregulatory influences, which at present are not understood but which clearly are quantitatively important in understanding regulation of apical membrane channel density. It became evident that mass law changes of channel density could be separated from those of autoregulatory influences by virtue of large differences in the time constants involved. This led in the design of the experiments to a pulse protocol that minimized time of inhibition of the I_{Na} where blocker-dependent changes of channel density would be due principally to those occurring by mass law action. According to a three-state scheme where blocker interacts alone with open channels, N_o^B was expected to decrease but to a lesser extent than would occur for two-state or four-state considerations ($N_o^B/N_o = 0.5$ at $B/K_B = 1.0$). Indeed, N_o^B/N_o was consistently >0.5 even at $[B] \gg K_B$. Moreover, it was observed consistently here as in previous experiments that N_{ob} increased with increasing $[B]$, indicating a blocker concentration-dependent recruitment of channels to open + blocked states. Hence, in pulse protocol experiments where autoregulatory influences on channel density are for all practical purposes absent, blocker-dependent recruitment of channels occurs from closed states of the channel. If so, it follows that blocker interacts primarily if not solely with open states of the channel. In this regard, as noted above, compelling evidence exists from experiments with amiloride that cationic blockers sense changes of membrane voltage and accordingly the suggestion has been made that blockers gain access to the open channels. This however does not preclude binding of blocker to the outside of the channel, but taken with the above observations it does suggest that such binding if it occurs is ineffective in altering the kinetics of the channels. If our view with regard to the long time-constant autoregulatory processes is correct, then it would be reasonable to believe that the acute blocker concentration dependence of channel densities can be ascribed to mass law action and is in accordance with a simple three-state model of blocker kinetics. This would explain the blocker-dependent changes of N_o^B and N_{ob} where recruitment of channels from closed into open and blocked states occurs at constant total channel density.

On the premise that N_T remained constant in pulse protocol experiments, the open probability was calculated at all $[B]$. It was observed that for all practical purposes, β' was essentially independent of $[B]$ despite relatively large changes of I_{Na} . In most groups of experiments, β' averaged near 0.4, and this value is remarkably similar to that reported for apical Na channels of rat distal tubules studied by patch clamp (Palmer and Frindt, 1986). Notably, β' varied widely among tissues ranging between ~ 0.1 and 0.9. A summary distribution of open probabilities is shown in Fig. 14, which emphasizes the idea that changes of open probability may in fact underlie an important mechanism by which epithelial cells regulate their Na entry. Rather little is yet known of the mechanism of control of open probability, although agents like benzoylimidazole-2-guanidine, diphenylhydantoin, and especially MK-196

(Merck, Sharp & Dohme) appear to increase the open probability (unpublished observations).

In all groups of experiments we calculated the expected blocker-dependent changes of N_o^B and N_{ob} assuming $N_T = N_T^B$ and β' were constant (independent of $[B]$ and independent of duration of inhibition of apical Na entry). These curves were superimposed as solid lines on the empirical measurements of N_o^B and N_{ob} . For pulse experiments, the empirical data conformed rather well with the expectation of this model, although as noted in the Results, small deviations from perfect behavior were observed at the higher $[B]$. Whether such deviations from ideal behavior indicate imperfection of the model or whether such deviations are due more likely to relatively small time-dependent increases of N_T^B cannot now be known with certainty. However, in view of the secondary transients of the I_{Na} , even in pulse experiments, the simplest explanation was to assume that deviations from ideal behavior were due most likely to long time-constant autoregulatory increases of N_T^B and not to changes of β' . Indeed, β' as determined in the microelectrode experiments indi-

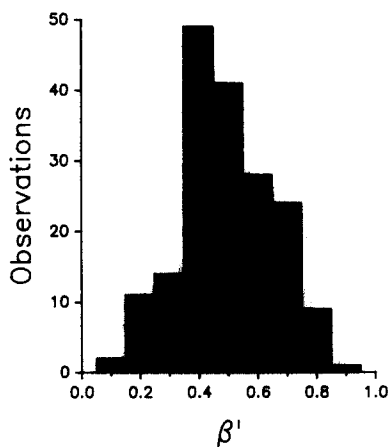


FIGURE 14. Frequency histogram of open-channel probabilities, β' , in the absence of blockers.

cated that open probability was not changed significantly by blocker inhibition of apical Na entry despite prolonged periods of inhibition of apical Na entry.

When staircase or time course protocols were used that necessarily involved prolonged durations of inhibition of apical Na entry, mean control values of β' were estimated from the extrapolated values of apparent " β " to the zero time and zero blocker concentration control state of the tissues. Done in this way, mean β' were similar for all groups of tissues. It should be emphasized here as above that values of apparent " β " calculated with Eq. 10 are subject to the assumption of constancy of N_T^B . With prolonged inhibition of apical Na entry, such an assumption did not appear valid. Indeed, in those experiments where CDPC was increased abruptly from 5 to 50 μM , N_{ob} was increased abruptly at first because of mass action of CDPC. The secondary long time-constant increase of N_{ob} reflected likely increases of N_T^B . Such behavior here as in other experimental groups with prolonged inhibition of apical Na entry would lead to time-dependent progressive decreases in calcu-

lation of the “ β ”. Having established the falling trend of “ β ”, the zero time and zero blocker concentration extrapolations of “ β ” at the ordinate should have provided reasonable estimates of the control open probability of the Na channels. From the results of both pulse and other protocols, we therefore conclude that both mass law action and autoregulatory processes contribute to changes of channel density where these processes are separable by differences in their time constants.

Autoregulatory Processes

Essentially nothing is known of the autoregulatory processes that influence apical membrane Na channel density nor the mechanisms that sense a change in the rate of apical Na entry. Our own experiments have so far been limited to blocker inhibition of Na entry. For this type of submaximal inhibition, autoregulatory processes are capable of returning the Na entry rate to near control values within 10–20 min so that the blocker does not appear to sustain mass law inhibition of Na entry. The reason for this appears to be a steady-state increase of the N_T with little or no measurable difference of open probability. After prolonged inhibition of I_{Na} , and where N_T was increased, abrupt removal of CDPC from the apical solution resulted in an overshoot of the I_{Na} which thereafter relaxed slowly towards original control values. Such observations are in accordance with the hypothesis of long time-constant changes of N_T and hence N_o after release of channels from steady-state blocker inhibition.

Amiloride

Determination of blocker-dependent changes of channel densities with amiloride is complicated by two factors. First, the threshold for detection of a Lorentzian component of the PDS occurs at $\sim 0.5 \mu\text{M}$ amiloride, which causes about an 80% inhibition of the I_{Na} . Accordingly, blocker-induced noise analysis can be done only in tissues where I_{Na} is reduced markedly from the spontaneous rates of Na transport and where extrapolation to control conditions is not reliable. Second, whereas the amiloride ON-rate coefficient (k_{ob}) is satisfactorily determined from the slope of the corner frequency plots, the amiloride OFF-rate coefficient (k_{bo}), owing to its very small value, is not measurable with sufficient precision to allow reasonable estimates of the K_B^{Amil} (Abramcheck et al., 1985; see footnote 3). Hence in the absence of a K_B^{Amil} determined this way, it was impossible to know the expected blocker-dependent mass law behavior of the channel densities.

We have in the measurement of the K_B^{Amil} taken advantage of the fact that K_B^{CDPC} is readily measured together with the fractional inhibitions of the I_{sc} caused by CDPC and amiloride. The important assumption was that fractional inhibition of the I_{sc} would be identical at the same $[B]/K_B$ for any blocker of the Na channels. K_B^{Amil} obtained this way averaged 61 nM for short-circuited epithelia bathed with Cl-HCO₃ Ringer solution of a pH of ~ 8.1 . For amiloride concentrations $< 0.4 \mu\text{M}$, K_B^{Amil} was independent of amiloride concentration. The experiments were carried out with a pulse protocol so that the time of inhibition of I_{sc} was the same for CDPC as for amiloride.

Because of differences of pH and apical membrane voltage between and among various preparations, it is difficult to compare directly values of K_B^{Amil} reported by

ourselves and others. However, it is clear that K_B^{Amil} measured macroscopically from changes of I_{sc} are >61 nM, usually falling into a range of a few hundred nanomolar amiloride. For example, in two groups of experiments reported by Helman et al. (1983), the apparent $K_{1/2}^{app}$ determined by analysis of Eadie-Hofstee plots (Engel, 1977; and Eq. 8 of Helman et al., 1983) averaged 207 and 269 nM. In such analyses the $\Delta I_{Na}/[B]$ is plotted against the ΔI_{Na} from which the slope yields the concentration of amiloride that causes a 50% reduction of the I_{Na} . If, however, inhibition of open channels is accompanied by recruitment of channels by mass law action from closed states at constant N_T , such macroscopic values of K_B^{Amil} must by necessity overestimate the microscopic K_B^{Amil} . It is easily shown for mass law action alone that:

$$\Delta I_{Na} = -(K_B/\beta')(\Delta I_{Na}/[B]) + \Delta I_{Na}^{max} \quad (18)$$

where the slope of the line is given by the microscopic K_B divided by the open probability. If we assumed as a first approximation the absence of autoregulatory changes of N_T , then with a K_B^{Amil} of 61 nM, β' for the two groups of experiments referred to above are in the vicinity of 0.31 and 0.25, respectively. With autoregulatory increases of N_T , these values are underestimates of the actual β' .

The implication from such reasoning according to three-state model kinetics is manifest in the interpretation of K_B obtained macroscopically from changes of I_{Na}^B . Certainly, changes of macroscopic K_B will reflect changes of either microscopic K_B and/or changes of β' . Thus it would seem prudent in the interpretation of changes of macroscopic values of K_B to keep in mind that open probability contributes importantly to its value and may at least in part be responsible for a change of macroscopic K_B when observed.

Epithelia were subjected to amiloride-induced noise analysis with both staircase and time course protocols. As expected, due to hyperpolarization of V_a , i_{Na} was increased on average by $\sim 30\%$, while I_{Na}^B was inhibited markedly at $[Amil] > 0.5 \mu M$. At this drug concentration, $[Amil]/K_B^{Amil}$ was 7.57 and was increased to a $[B]/K_B$ of 151.5 at $10 \mu M$ amiloride. Obviously, it was not advantageous to investigate blocker-dependent changes of channel densities in this range of B/K_B . Nevertheless, as indicated in Figs. 12 and 13, the expected changes of N_o^B and N_{ob} from mass law action were remarkably the same as expected for control open probabilities that averaged 0.45 and 0.50 for both groups of experiments at $0.5 \mu M$, and for which time of inhibition of I_{Na} was minimal. Autoregulatory changes of N_o^B and N_{ob} were also observed in both groups of experiments, although here, in comparison with CDPC, the time-dependent changes of channel densities were considerably larger, due most likely to the far greater inhibition of I_{Na} over similar time intervals than those encountered with CDPC. Thus, in pragmatic terms, the behavior of the tissues was the same qualitatively despite quantitative differences in response to blocker inhibition of Na entry. If we accept the idea of a three-state model with β' of 0.45 for the experiments of Fig. 12, then as shown in Fig. 12 C, recruitment from closed into open and blocked states by mass action alone should have "saturated" the N_{ob} at amiloride concentrations $> 1-2 \mu M$. This however was not observed. Rather, N_{ob} was increased markedly above expected values. This is attributable to autoregulatory processes where channels are recruited from other than closed states of the channel, possibly from dormant channels within apical membranes or from channel-con-

taining vesicles inserted into apical membranes from stored sites within the cytoplasm.

It should be emphasized again that the three-state model adopted here deals alone with mass law effects that occur on a time scale of seconds as dictated by the rate coefficients α , β , k_{ob} , and k_{bo} . Clearly, additional states of the Na channel must exist that influence N_T , thereby contributing to autoregulatory, hormonal, and other mechanisms of regulation of channel densities that must be capable of changing N_T . No unique insights into these additional states have emerged from the present investigation. Although open probability varies markedly among tissues, inhibition of I_{Na} by either CDPC or amiloride did not appear to affect β' , and thus the newly recruited channels would seem to possess the same β' as the older channels. Accordingly, differences of open probability are not likely to be related to the age of the channels.

Supported by National Institutes of Health grants DK-16663 and DK-30824. Dr. Baxendale was an American Heart Association (Illinois affiliate) fellow during part of this project.

We are grateful to Nancy Suarez and John Waters for excellent technical assistance and to Dr. Alvin Essig and Dr. David Dawson for helpful suggestions during the preparation of this manuscript. We are also grateful to Dr. Yoshinori Marunaka and Dr. Douglas C. Eaton for allowing us to read a preprint of their manuscript (Marunaka, Y., and D. C. Eaton, manuscript submitted for publication).

Original version received 17 April 1989 and accepted version received 11 September 1989.

REFERENCES

- Abramcheck, F. J., W. Van Driessche, and S. I. Helman. 1985. Autoregulation of apical membrane Na^+ permeability of tight epithelia. Noise analysis with amiloride and CGS 4270. *Journal of General Physiology*. 85:555–582.
- Baxendale, L. M., and S. I. Helman. 1986. Sodium concentration dependence of apical membrane single channel Na^+ current and density of nondepolarized frog skin (three state model). *Biophysical Journal*. 49:106a. (Abstr.)
- Eaton, D. C., and K. L. Hamilton. 1988. The amiloride-blockable sodium channel of epithelial tissue. In *Ion Channels*. Vol. 1. T. Narahashi, editor. Plenum Publishing Corp., New York. 251–282.
- Engel, P. C. 1977. *Enzyme Kinetics of the Steady State Approach*. Chapman & Hall, London. 96 pp.
- Goldman, D. E. 1943. Potential, impedance, and rectification in membranes. *Journal of General Physiology*. 69:571–604.
- Helman, S. I., T. C. Cox, and W. Van Driessche. 1983. Hormonal control of apical membrane Na transport in epithelia. Studies with fluctuation analysis. *Journal of General Physiology*. 82:201–220.
- Helman, S. I., and R. S. Fisher. 1977. Microelectrode studies of the active Na transport pathway of frog skin. *Journal of General Physiology*. 69:571–604.
- Helman, S. I., B. M. Koeppen, K. W. Beyenbach, and L. M. Baxendale. 1985. Patch clamp studies of apical membranes of renal cortical collecting ducts. *Pflügers Archiv*. 405(Suppl. 1):S71–S7.
- Ilani, A., S. Yachin, and D. Lichtstein. 1984. Comparison between bretylium and diphenylhydantoin interaction with mucosal sodium-channels. *Biochimica et Biophysica Acta*. 777:323–330.

- Li, J. H.-Y., E. J. Cragoe, Jr., and B. Lindemann. 1985. Structure-activity relationship of amiloride analogs as blockers of epithelial Na channels. I. Pyrazine-ring modifications. *Journal of Membrane Biology*. 83:45–56.
- Li, J. H.-Y., E. J. Cragoe, Jr., and B. Lindemann. 1987. Structure-activity relationship of amiloride analogs as blockers of epithelial Na channels. II. Side-chain modifications. *Journal of Membrane Biology*. 95:171–185.
- Li, J. H.-Y., and B. Lindemann. 1983. Competitive blocking of epithelial sodium channels by organic cations: the relationship between macroscopic and microscopic inhibition constants. *Journal of Membrane Biology*. 76:235–251.
- Palmer, L. B. 1984. Voltage-dependent block by amiloride and other monovalent cations of apical Na channels in the toad urinary bladder. *Journal of Membrane Biology*. 80:153–165.
- Palmer, L. G., and G. Frindt. 1986. Amiloride-sensitive Na channels from the apical membrane of the rat cortical collecting tubule. *Proceedings of the National Academy of Sciences*. 83:2767–2770.
- Rick, R., A. Dörge, E. von Arnim, and K. Thureau. 1978. Electron microprobe analysis of frog skin epithelium: evidence for a syncytial sodium transport compartment. *Journal of Membrane Biology*. 39:313–331.
- Sariban-Sohraby, S., R. Latorre, M. Burg, and D. Benos. 1984. Amiloride-sensitive epithelial Na⁺ channels reconstituted into planar lipid bilayer membranes. *Nature*. 308:80–82.
- Stoddard, J. S., and S. I. Helman. 1985. Dependence of intracellular Na⁺ concentration on apical and basolateral membrane Na⁺ influx in frog skin. *American Journal of Physiology*. 249:F662–F671.
- Warncke, J., and B. Lindemann. 1985. Voltage dependence of Na channel blockage by amiloride: relaxation effects in admittance spectra. *Journal of Membrane Biology*. 86:255–265.
- Van Driessche, W., and W. Zeiske. 1980. Ba²⁺-induced conductance fluctuations of spontaneously fluctuating K⁺ channels in the apical membrane of frog skin (*Rana temporaria*). *Journal of Membrane Biology*. 56:31–42.